Experimental Study of Flow Boiling Heat Transfer in a Horizontal Microfin Tube

Yu, Jian
Institute of Advanced Material Study, Kyushu University

Koyama, Shigeru
Institute of Advanced Material Study, Kyushu University

Momoki, Satoru
Faculty of Engineering, Nagasaki University

https://doi.org/10.15017/6669

出版情報：九州大学機能物質科学研究所報告. 9 (1), pp.27-42, 1995-11-15. 九州大学機能物質科学研究所
バージョン：
権利関係：

機能物質科学研究所
報告 第9巻 第1号
pp. 27～42(1995)

Experimental Study of Flow Boiling Heat Transfer in a Horizontal Microfin Tube

Jian YU, Shigeru KOYAMA, and Satoru MOMOKI[1]

An experimental study on flow boiling heat transfer in a horizontal microfin tube is conducted with pure refrigerants HFC134a, HCFC123 and HCFC22 using a water-heated double-tube type test section. The test microfin tube is a copper tube having the following dimensions: 8.37mm mean inside diameter, 0.168mm fin height, 60 fin number and 18 degree of helix angle. The local heat transfer coefficients for both counter and parallel flows are measured in a range of heat flux of 1 to 93W/m^2, mass velocity of 100 to 395kg/(m^{2}s) and reduced pressure of 0.07 to 0.21. The experimental data are tabled and compared with several existing correlations.

Recently, different kinds of microfin tubes with high heat transfer performance and relatively low flow resistance are widely used in heat pump and air conditioning systems. In designing the optimum systems, the heat transfer and flow resistance characteristics in microfin tubes should be clarified. The flow boiling in microfin tubes has been experimentally studied by many investigators. Among of them, Ito-Kimura[1)], Khanpara et al.[2)] and Kido-Uehara[3)] tested many kinds of microfin tubes and obtained a lot of first-hand heat transfer data; Yoshida et al.[4)] and Fujii et al.[5)] observed directly the flow pattern in microfin tubes; Miyara et al.[6)], Kandlikar[7)], Murata-Hashizume[8)] and Kido-Uehara[3)] proposed correlation equations for the flow boiling heat transfer coefficient in microfin tubes, respectively, but these proposed equations are only valid for their test ranges.

In the present paper, an experimental study of flow boiling heat transfer in a microfin tube is carried out using three kinds of pure refrigerants HFC134a, HCFC123 and HCFC22 as test fluid. The experimental data are compared with several previous correlations including authors' correlation[9)] and tabulated for the common reference.

Nomenclature

A heat transfer area per unit length of test tube [m^2/m]
Cp isobaric specific heat [$J/(kg\ K)$]
d_i mean inside diameter [m]
d_o outside diameter [m]
d_r root diameter [m]
d_t tip diameter [m]
G mass velocity [$kg/(m^2\ s)$]

Received July 5, 1995
Dedicated to Professor Hiroshi Kobayashi on the occasion of his retirement
[1]Faculty of Engineering, Nagasaki University, Nagasaki, Japan

h enthalpy [J/kg]
h_{lsat} saturated liquid enthalpy [J/kg]
h_{vsat} saturated vapor enthalpy [J/kg]
h_t fin height [m]
L length of test section [m]
n fin number
P pressure [MPa]
p fin pitch [m]
P_c critical pressure [MPa]
P_r reduced pressure, $=P/P_c$
Q total heat transfer rate [W]
q heat flux [W/m^2]
s fin tip width [m]
T temperature [K]
t temperature [°C]
W mass flow rate [kg/h]
w fin valley width [m]
x quality
Z distance [m]
ΔL effective heating length of one subsection [m]
α heat transfer coefficient [$W/(m^2\ K)$]
γ helix angle [degree]
λ thermal conductivity [$W/(m\ K)$]
μ dynamic viscosity [$Pa\ s$]
ξ dimensionless parameter defined by Eq.(8)
ξ_A ratio of inside surface area between microfin and smooth tubes
ρ density [kg/m^3]
σ surface tension [N/m]
ψ dimensionless parameter defined by Eq.(9)

Subscripts

air air
b bulk, or bottom of test tube
C,cal calculated
exp experimental
i inside surface of test tube
in inlet
l liquid, or left side of test tube
M measured
m mean
o outside surface of test tube
out outlet
R refrigerant
r right side of test tube
RC bulk refrigerant
S heating water
s,sat saturated
t top of test tube

total	total heat transfer surface
v	vapor
W	tube wall
water	water

Experimental Apparatus

Test loop. The experimental apparatus used in this study is shown in Fig.1. It consists of three main loops: a refrigerant loop, a water loop and a brine loop. In the refrigerant loop, the subcooled liquid refrigerant is delivered with a pump(1) through a desiccant filter(2), a mass flow meter(3), an electrical preheater(4), a mixing chamber(5) and a heat exchanger (6) to the test section(10) or (11). The refrigerant vapor generated in the test section

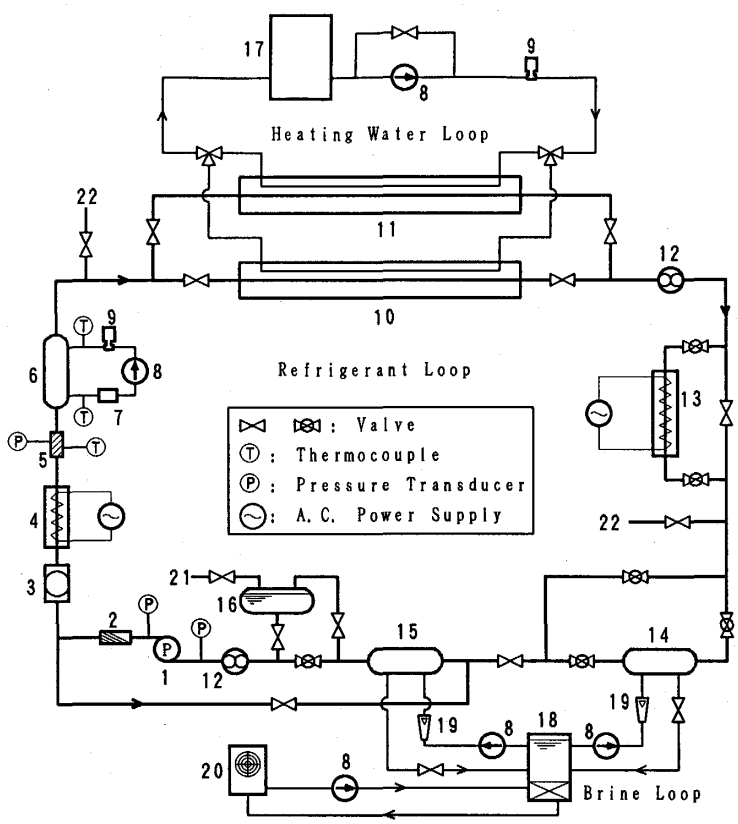

1	Positive displacement pump	12	Sight glass
2	Desiccant filter	13	After-heater
3	Mass flow meter	14	Condenser 1
4	Preheater	15	Condenser 2
5	Mixing chamber	16	Liquid reservoir
6	Heat exchanger	17	Heat source tank
7	Heat sink tank	18	Brine tank
8	Centrifugal pump	19	Float-type flow meter
9	Gear-type flow meter	20	Chilling unit
10	Test section(Smooth tube)	21	Charging port
11	Test section(Microfin tube)	22	Sampling port

Figure 1 Experimental apparatus.

condenses in two condensers(14) and (15) to complete the cycle. The pump(1) used in the refrigerant loop is a positive-displacement pump, that was used instead of a compressor to eliminate the effect of lubricating oil. The desiccant filter(2) is used to exclude the water dissolved in the refrigerant. The electrical preheater(4) and the heat exchanger(6) are used to adjust the thermodynamic state of refrigerant at the entrance of the test section. The after -heater(13) is used to control the pressure in the refrigerant loop. The water loop, including a heat source tank(17), a centrifugal pump(8) and a gear-type flow meter(9), is used to supply heating water to the test section. The brine loop, which consists of a brine tank(18), a chilling unit(20), two centrifugal pumps(8) and two float-type flow meters(19), is used to condense the refrigerant. The temperature in the brine tank is usually set at -2°C in the flow boiling experiments.

Test section. The test section shown in Fig. 2 is a horizontal double-tube heat exchanger in which the refrigerant flows inside the inner tube and the heating water flows in the annulus. The inner tube is a straight microfin copper tube. The outer tube is formed by two polycarbonate resin blocks each of which has a half-round ditch with a radius of 8mm; so the dimension of the annular gap for a water flow is 3mm. To measure the local heat transfer rate, the annulus is divided into 14 subsections along the tube axis by partition blocks. The heat transfer rate in each subsection is treated as a local value. In these subsections, No.1, 2, 13, and 14 subsections are of 250mm long, half length of the others. Depending on the requirement of the experiments, the flow condition in the double-tube heat exchanger can be

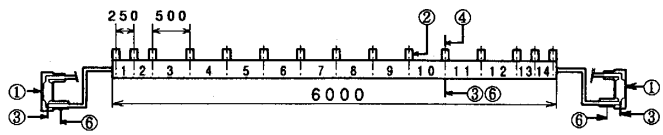

(a) Schema of test section

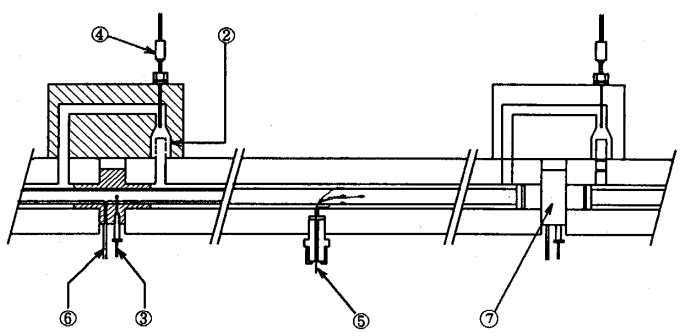

(b) Detail of subsection

1 Mixing chamber(Refrigerant)
2 Mixing chamber(Heating water)
3 Thermocouple(Refrigerant)
4 Resistant thermometer(Heating water)
5 Thermocouple(Tube surface)
6 Pressure measuring port
7 Partition block

Figure 2 Test section.

Table 1 Details of test section.

Type		Double-tube heat exchanger	
Material	Inside tube	Copper	
	Outside tube	Polycarbonate	
i.d. of outside tube		16.0[mm]	
o.d. of inside tube		10.0[mm]	
Mean i.d. of inside tube		8.37[mm]	
Length of test section		6000[mm]	
Length of developing region		600[mm] for both ends	
Subsection	Number	10	4
	Length	500[mm]	250[mm]
	Heating length	460[mm]	210[mm]
Pass	Refrigerant side	Inside tube	
	Water side	Annulus	
Flow condition		Counter or Parallel	

set to counter flow or parallel flow by means of valves in the refrigerant loop. Details of the test section are listed in the Table 1.

Test Tube. The geometrical parameters of the copper microfin tube are summarized in Table 2, and the cross section, side view and fin profile of the tube are shown in Fig. 3. The microfin tube is of 6.0m in length, 10.0mm in outside diameter and 8.37mm in mean inside diameter, with which the cross-sectional area of a smooth tube equals to that of the microfin tube. The thermal conductivity of the tube is 385W/(m K).

Measurement method. The pressure and temperature sensors arranged in the test section are indicated in Fig. 2. The absolute pressure at the entrance of the test section is measured with two absolute pressure transducers. The pressure drop for every three continuous subsections is measured with a differential pressure transducer. The pressure drop in each subsection is obtained from the interpolation of the measured data. The heating water temperatures are measured with fifteen 2.0mm o.d. resistance thermometers (Pt 100 Ω) inserted in the mixing chambers at the inlets of all subsections and the exit of the test section. The bulk temperatures of refrigerant are measured with two 0.5mm o.d. K-type thermocouples inserted in the mixing chambers at the both ends of the test section. The refrigerant temperatures are measured with fifteen 0.5mm o.d. K-type thermocouples inserted into the test tube at the partition blocks. The wall temperatures of the test tube are measured at the center of each

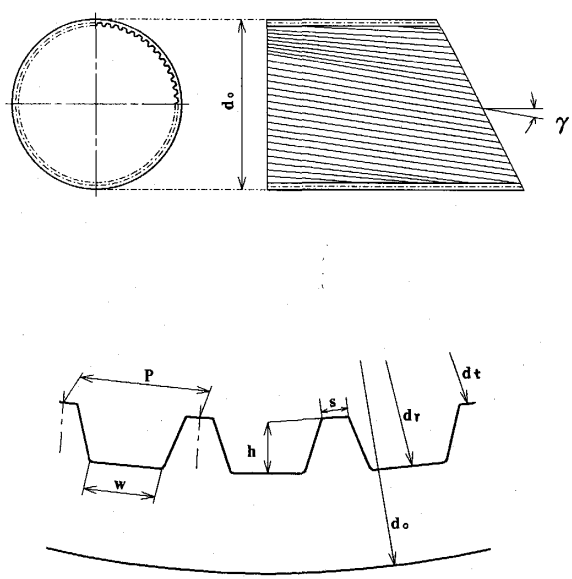

Figure 3 Cross section, side view and fin profile of microfin tube.

Table 2 Dimensions of microfin tube.

Outside diameter	d_o[mm]	10.00
Mean i.d.	d_i[mm]	8.37*
Root i.d.	d_r[mm]	8.475
Tip i.d.	d_t[mm]	8.139
Fin height	h_t[mm]	0.168
Fin pitch	p[mm]	0.44
No. of fins	n[−]	60
Helix angle	γ[mm]	18
Tip width	s[mm]	0.073
Valley width	w[mm]	0.245
Tip geometry		flat
Valley geometry		flat
A_{avg}/A_{smooth}		1.52

* The mean inside diameter for the microfin tube is an averaged value, with which the cross-sectional area of a smooth tube is equal to that of the microfin tube.

subsection with four 0.1mm o.d. T-type thermocouples, which are attached at the top, both sides and bottom of the outside surface of the tube.

As shown in Fig. 1, the refrigerant flow rate is measured with a mass flow meter, and the heating water flow rate is with a gear-type flow meter.

The sensors used in the present experiments and their accuracy are summarized in Table 3.

Table 3 Sensors used in the present study.

Measured quantity and location		Sensor	Uncertainty
Temperature	Refrigerant temp. in mixing chambers at both ends of test section	ϕ0.5 K-type T.C.	0.11[°C]
	Refrigerant temp. at inlet and outlet of each subsection		
	Room temp.		
	Water temp. in mixing chambers at both ends of each subsection	ϕ2.0 R.T.(Pt100Ω)	0.014[°C]
	Outside wall temp.	ϕ0.1 T-type T.C.	0.18[°C]
Flow Rate	Refrigerant	Mass flow meter	1.5[kg/h]
	Heating water	Gear-type flow meter	3[kg/h]
Pressure	Absolute pressure at entrance	Absolute P.T. (PA20KB)	1.96[kPa]
		Absolute P.T. (PA10KB)	0.98[kPa]
	Pressure drop	Differantial P.T. (PD200GA)	0,19[kPa]

T.C.: thermocouple, R.T.: resistance thermometer, P.T.: pressure transducer.

Data Reduction

The heat transfer rate at each subsection, Q_S, is calculated from

$$Q_S = W_S C_{PS} (T_{S,in} - T_{S,out}) \tag{1}$$

where W_S is the flow rate of heating water, $T_{S,in}$ and $T_{S,out}$ are the heating water temperatures at the inlet and outlet of each subsection, respectively, and C_{PS} is the isobaric specific heat of water at the average temperature $(T_{S,in} + T_{S,out})/2$. In the test section the annular side is divided into 14 subsections by partition blocks, as shown in Fig. 2. Therefore, the effective heating length is 210mm for No.1,2,13 and 14 subsections, and 460mm for the others. This effective heating length is used in data reduction for the heat transfer characteristics. Because of the heat loss to ambient air, modification of the heat transfer rate is necessary to evaluate the heat transfer coefficient. Based on a series of preliminary tests, the following correlation was developed to evaluate the real heat transfer rate in the refrigerant side Q_R.

$$Q_R = Q_S - 0.3848\left(\frac{T_{S,in} + T_{S,out}}{2} - T_{air}\right)\Delta L \tag{2}$$

where T_{air} is the room temperature and ΔL is the effective heating length of one subsection.

For the microfin tube the heat flux q, which is based on the real inside surface area of the tube that includes the base and the fin areas, is defined as

$$q = \frac{Q_R}{\xi_A \pi d_i \Delta L} \tag{3}$$

where d_i is the mean inside diameter of the microfin tube, and ξ_A is the ratio of the real inside surface area of the microfin tube to the inside surface area of a smooth tube with a diameter d_i.

The inside surface temperature of the test tube in each subsection, T_{Wi}, is obtained from the measured outside surface temperature using the radial heat conduction equation,

$$T_{Wi} = T_{Wo} - \frac{Q_R}{2\pi\lambda_W \Delta L} \ln\left(\frac{d_o}{d_i}\right) \tag{4}$$

where T_{Wo} is the average outside surface temperature, d_o is the outer diameter of the tube, and λ_W is the thermal conductivity of the tube(=385W/(m K)).

The bulk refrigerant temperature and the quality are calculated at the inlet, outlet and center of each subsection under the assumption of a uniform temperature distribution in both liquid and vapor phases at a cross section. In the case of subcooled condition at the entrance, the calculation procedure is as follows:

1. The bulk enthalpy at the entrance is calculated using the measured pressure and temperature in the refrigerant mixing chamber.
2. Using the calculated enthalpy at the entrance and the heat transfer rate in each subsection, the outlet bulk enthalpy at each subsection is successively calculated as

$$h_{b,out} = h_{b,in} + Q_R / W_R \tag{5}$$

where h_b is the bulk specific enthalpy of a cross section. The subscripts *in* and *out* mean the inlet and outlet, respectively. The bulk enthalpy at the center of each subsection is assumed as the average value of the inlet and outlet enthalpy.

3. The enthalpy of saturated liquid and vapor at the inlet and outlet of each subsection is obtained from the equation of state using the measured pressure. The enthalpy of saturated liquid and vapor at the center of each subsection is also calculated with the average pressure between the inlet and outlet. If the bulk enthalpy is lower than the saturated liquid value, the refrigerant is assumed to be in subcooled liquid state. In

contrast, as the bulk enthalpy is higher than the saturated vapor value, the refrigerant is assumed to be in superheated vapor state. When the bulk enthalpy is between the saturated liquid and saturated vapor enthalpy, the bulk temperature is set to the saturated temperature, while in the subcooled or superheated region the bulk temperature is calculated from the equation of state using the bulk enthalpy and measured pressure.

4. In the saturated region the quality at the inlet, outlet and center of each subsection is obtained from the following equation.

$$x=\frac{h_b-h_{lsat}}{h_{vsat}-h_{lsat}} \tag{6}$$

where h_{lsat} and h_{vsat} are the enthalpy of saturated liquid and vapor, respectively. In the subcooled region the value of x is forced to 0, while in the superheated region it is fixed to 1.

In the case of saturated condition at the entrance, the above calculation is successively proceeded from the exit of the test section where the refrigerant is in superheated vapor state.

The heat transfer coefficient for the microfin tube is defined as

$$\alpha=\frac{q}{T_{Wi}-T_{RC}} \tag{7}$$

where T_{RC} is the calculated bulk temperature at the center of a subsection.

The thermophysical properties for the pure refrigerants are calculated according to the thermophysical property tables of refrigerants by JAR[10,11].

Results and Discussion

The ranges of experimental parameters are listed in Table 4. The heat flux ranges from 1 to 93W/m², mass velocity of 100 to 395kg/(m²s) and reduced pressure of 0.07 to 0.21 for counter and parallel flow conditions. For the reference, some sets of experimental data are tabled in Appendix.

Table 4 Experimental ranges.

(a) Counter flow.

Refrigerant	G_R	$P_{R,in}$	x	q
	kg/m²s	MPa	-	kW/m²
R134a	100~357	0.63~0.71	0~1	2~93
R123	113~330	0.25~0.46	0~1	4~93
R22	105~395	0.56~1.22	0~1	1~65

(b) Parallel flow.

Refrigerant	G_R	$P_{R,in}$	x	q
	kg/m²s	MPa	-	kW/m²
R134a	120~360	0.56~0.68	0~1	4~93
R123	141~293	0.25~0.31	0~1	2~46
R22	200~312	1.09~1.11	0~1	4~58

Figures 4 (a) and (b) show examples of the temperature distribution along the tube from the inlet of refrigerant under the counter and parallel flow conditions, respectively. The symbols △, ▽, ◇ and ○ denote the measured temperature of refrigerant T_{RM}, the calculated bulk temperature of refrigerant T_{RC}, the inside surface temperature T_{Wi} and the temperature of heating water T_S, respectively. The heat flux q and the vapor quality x are also plotted in these figures by symbols ● and ×, respectively. In the case of counter flow, the refrigerant temperature increases in the flow direction until it researches saturated temperature, then it decreases gradually due to the pressure drop. In the saturated region, the measured temperature T_{RM} is in good agreement with the calculated bulk temperature T_{RC}. This indicates that the measured refrigerant pressure is very reliable. As the quality x is over about 0.9, the wall temperature T_{Wi} increases sharply, which indicates that the dryout happens in the tube. The temperature difference between refrigerant and water increases with the progression of boiling, and so does the heat flux before the dryout point. In the case of parallel flow, the temperature difference between refrigerant and water and the heat flux decreases in the direction of refrigerant flow. Near the dryout point the wall temperature only increases a little unlike that in the counter flow condition.

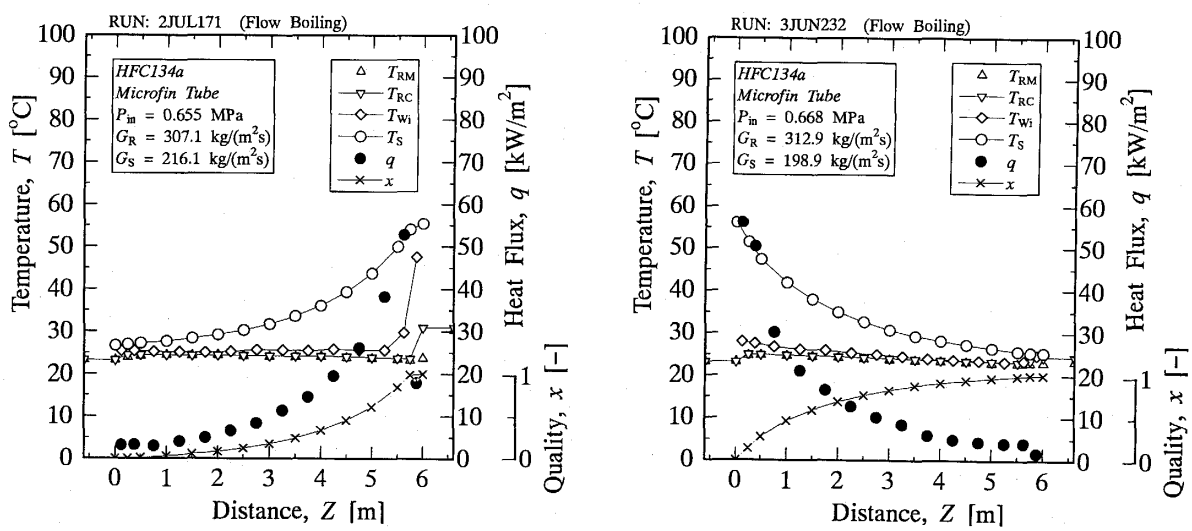

(a) Counter flow. (b) Parallel flow.

Figure 4 Axial distributions of temperatures, heat flux and quality (HFC134a).

As the flow pattern is not observed in the present study, it is classified referring to the experimental results of Fujii et al.[5] in a microfin tube plotted on the modified Baker's map[12]. Their results were obtained from direct observation through sight glasses. The present results of three kinds of pure refrigerants in counter flow condition are shown in Fig. 5. In this figure ξ and ψ are dimensionless parameters defined as

$$\xi=\left[\left(\frac{\rho_v}{\rho_{air}}\right)\left(\frac{\rho_l}{\rho_{water}}\right)\right]^{1/2} \tag{8}$$

$$\psi=\frac{\sigma_{water}}{\sigma}\left[\left(\frac{\mu_l}{\mu_{water}}\right)\left(\frac{\rho_{water}}{\rho_l}\right)^2\right]^{1/2} \tag{9}$$

where the subscripts air and water mean the physical properties of air and water at the standard condition (20°C, 1atm), respectively, and σ_{water} is the surface tension between water and air. Compared with the results of Fujii et al., it is inferred that most of the present data are located in the wavy-annular or annular flow region, even in the low mass velocity condition.

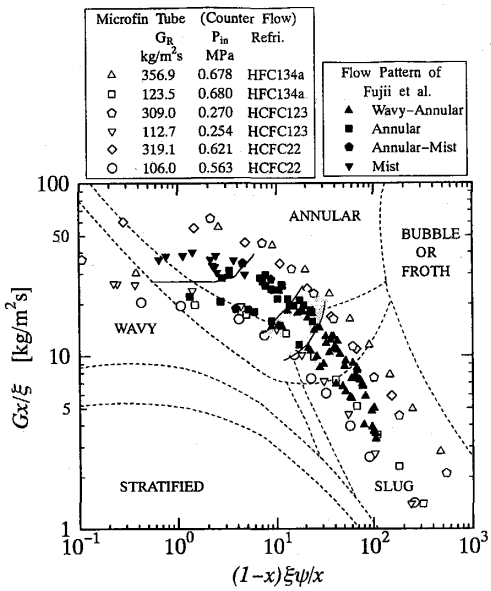

Figure 5 Flow pattern in microfin tubes.

Figures 6(a), (b), (c) and (d) show the typical results of circumferential distribution of the outside surface temperature T_{wo} against the quality x. In these figures the symbols △, □, ○ and ▽ denote the measured values at the top, right side,left side and bottom, respectively. T_{wm} denoted by a solid line is a circumferentially averaged value of T_{wo}. The calculated bulk temperature of refrigerant T_{RC} is also denoted by a broken line in these figures. It is found in these figures that in high mass velocity cases the circumferential variation of T_{wo} is small in the range of $0.1<x<0.8$, which may correspond to the wavy-annular or annular flow region. In low mass velocity cases it is also small in the range of $0.1<x<0.8$.

In the present study, only the experimental data satisfying the following conditions are treated: $0.1<x<0.8$, $|T_{wo}-T_{wm}|<0.5K$ and

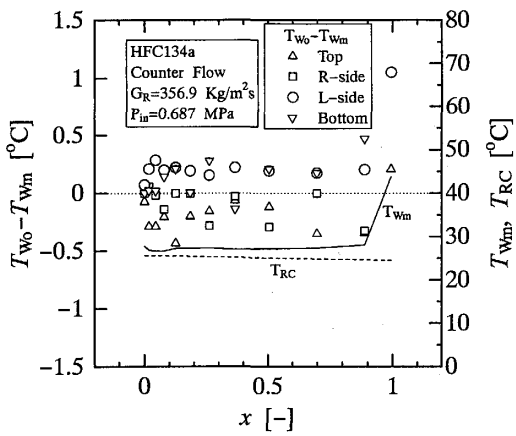

(a) High mass velocity (Counter flow).

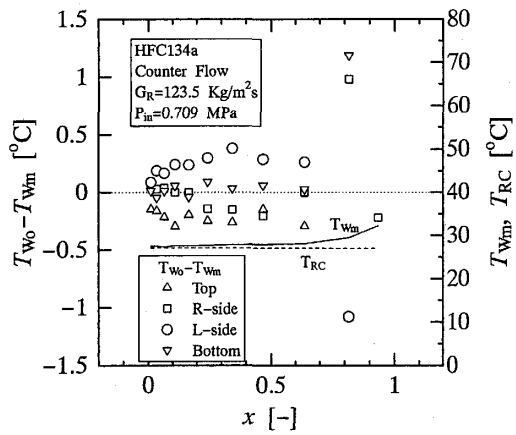

(b) Low mass velocity (Counter flow).

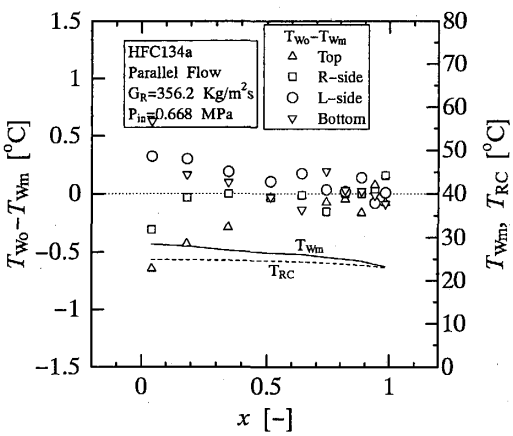

(c) High mass velocity (Parallel flow).

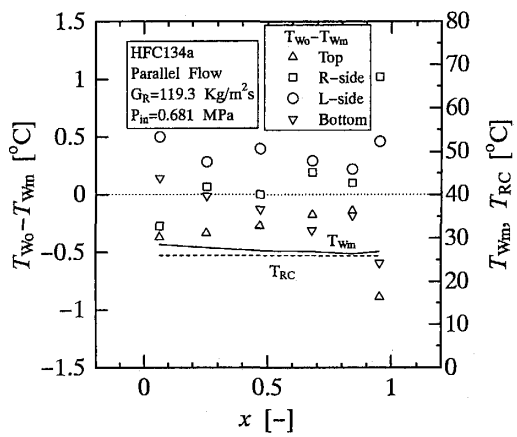

(d) Low mass velocity (Parallel flow).

Figure 6 Axial distribution of wall temperatures.

$(T_{Wi}-T_{RC})>1.0K$. The first and second conditions are used to select the data in the wavy -annular or annular flow region. The third one is to avoid large measurement error in the heat transfer coefficient.

Until now, only a few experimental correlations have been proposed to predict the flow boiling heat transfer coefficient in microfin tubes. However, most of these correlations were developed only based on a few kinds of microfin tubes and a few kinds of refrigerants. To confirm whether these correlations can be applied for other kinds of microfin tubes and other kinds of refrigerants or not, the comparison between the present data and previous correlations is carried out here.

Figures 7(a), (b), (c) and (d) show the comparison between the present data and the correlations of Kandlikar[7], Kido-Uehara[3], Miyara et al.[6] and Murata-Hashizume[8], respectively. In Kandlikar's correlation the heat transfer coefficient is defined based on the real inside surface area and the maximum inner diameter of microfin tube. Kido-Uehara used the similar definition to Kandlikar's except for the mean inside diameter d_i. Miyara et al. and Murata-Hashizume correlated their experimental data based on a mean inside diameter and an inside surface area of $\pi d_i \Delta L$. It is found that for the data of HFC134a and HCFC22 with high heat flux Kandlikar's correlation gives a relatively good agreement, while for the HCFC123 data and some data of HFC134a and HCFC22 with low heat flux his correlation gives overprediction. The reason is that in his correlation the convective heat transfer

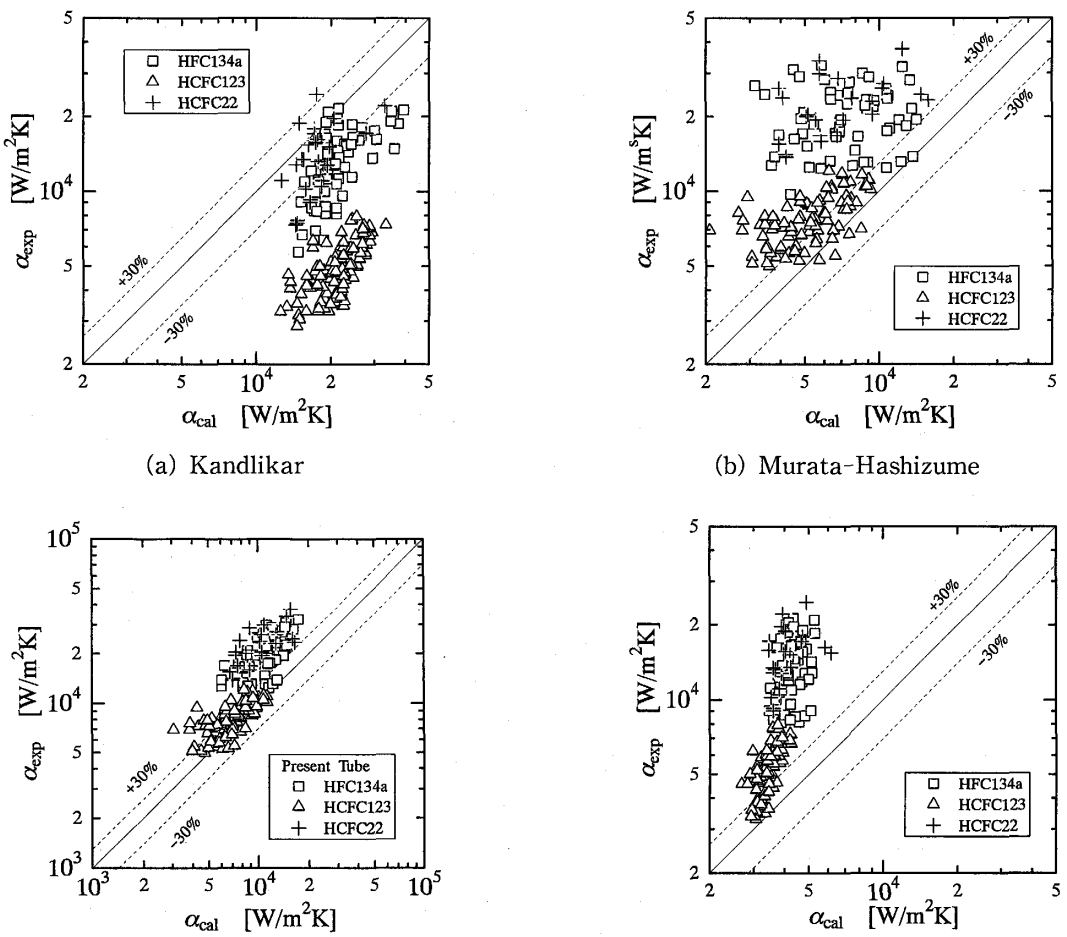

(a) Kandlikar

(b) Murata-Hashizume

(c) Miyara et al.

(d) Kido-Uehara

Figure 7 Comparison of present data with several previous correlations.

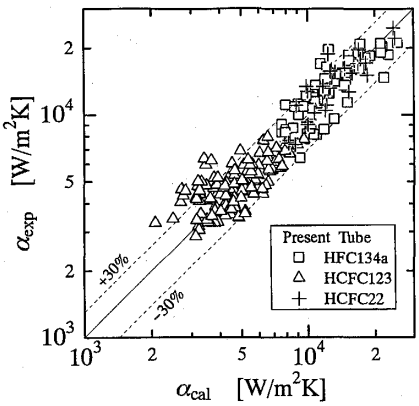

Figure 8 Comparison of the experimental data with authors' correlation.

component, which is dominant at low heat flux condition, is overestimated. On the other hand the values predicted by the correlation of Kido-Uehara is lower than most of the present data. This reason is that in their correlation the nucleate boiling component may be underpredicted. Comparison between the correlation of Miyara et al. for HCFC22 and the present data shows that the prediction is in good agreement with the data of HFC134a and HCFC123, but is lower in some degree for the data of HCFC22 in high heat flux region. The Murata-Hashizume correlation agrees with only some HCFC123 data, but underpredicts for the data of HFC134a and HCFC22. This reason is that their correlation was developed only using the experimental data of HCFC123 at a pressure of 0.2MPa; at this pressure the nucleate boiling contribution of HCFC123 is very weak.

From the above comparison, it is found that the previous correlations can not be applied for the present experimental data. Considering the effects of the differences between microfin surface and smooth surface, and modifying the correlation for smooth tube[13], the following correlation was developed for the flow boiling heat transfer in a microfin tube by authors[9].

$$\alpha=\alpha_{cv}+\alpha_{nb} \tag{10}$$

where

$$\alpha_{cv}=0.028Re_{tp}^{0.8}\,Pr_l^{0.4}\left(\frac{\lambda_l}{d_i}\right) \tag{11}$$

$$Re_{tp}=F^{1/0.8}\,Re_{lo} \tag{12}$$

$$Re_{lo}=\frac{G(1-x)d_i}{\mu_l} \tag{13}$$

$$F=1+2\left(\frac{1}{X_{tt}}\right)^{-0.88}+0.8\left(\frac{1}{X_{tt}}\right)^{1.03} \tag{14}$$

$$\alpha_{nb}=K^{0.745}S\alpha_{pb} \tag{15}$$

$$K^{0.745}=\frac{1}{1+0.875\eta+0.518\eta^2-0.159\eta^3+0.7907\eta^4} \tag{16}$$

$$\eta=\frac{\alpha_{cv}}{S\alpha_{pb}} \tag{17}$$

$$S=\frac{1}{\xi}(1-e^{-\xi}) \tag{18}$$

$$\xi=\frac{D_b\alpha_{cv}}{\lambda_l} \tag{19}$$

$$D_b=1.0\times10^{-5}\times\left(\frac{\rho_l}{\rho_v}\frac{Cp_l}{h_{fg}}T_{sat}\right)^{1.25}\left(\frac{2\sigma}{g(\rho_l-\rho_v)}\right)^{0.5} \tag{20}$$

$$\alpha_{pb}=2.8\times207\frac{\lambda_l}{D_{be}}\left(\frac{qD_{be}}{\lambda_l T_{sat}}\right)^{0.745}\left(\frac{\rho_v}{\rho_l}\right)^{0.581}Pr_l^{0.533} \tag{21}$$

$$D_{be}=0.51\sqrt{\frac{2\sigma}{g(\rho_l-\rho_v)}} \tag{22}$$

Figure 8 shows the comparison between the present experimental data and the Eq.(10). The predicted values are in good agreement with the experimental data, where the mean and average deviation are 12% and -0.8%, respectively.

Conclusions

An experimental study on the flow boiling heat transfer in a microfin tube were performed under both the counter flow and the parallel flow conditions using three kinds of refrigerants HFC134a, HCFC123 and HCFC22. The apparatus, measurement method and data reduction method used in the present study were described in detail. The ranges of the correlated data are G_R=200~360 $kg/(m^2\ s)$, P=0.25~1.11 MPa and q=5~64 $kW/(m^2\ K)$. Although there are several published correlations for the flow boiling heat transfer in microfin tubes, these correlations can not predict well the present experimental data. A new correlation proposed by authors agrees well with the present experimental data in wavy-annular and annular flow regions within the absolute deviation of 12%.

References

1) M.Ito and H.Kimura, *Trans. Jpn. Soc. Mech. Eng.*, **45, 389**, p.118 (1979.)
2) J.C.Khanpara, M.B.Pate and A.E.Bergles, *ASME Trans. HTD.*, **85**, p.31 (1987).
3) O.Kido and H.Uehara, *Trans. of the JAR*, **11**, **2**, p.730 (1994).
4) S.Yoshida, T.Matusnaga, H-P.Hong and K.Nishikawa, *Bulletin of JSME*, **31, 3**, p.505 (1988).
5) T.Fujii, S.Koyama, N.Inoue, K.Kuwahara and S.Hirakuni, *Trans. Jpn. Soc. Mech. Eng.*, **59, 562**, p.261 (1993).
6) A.Miyara, H.Takamatsu, S.Koyama, K.Yonemoto and T.Fujii, *Trans. Jpn. Soc. Mech. Eng.*, **54, 505**, p.2523 (1988).
7) S.G.Kandlikar, *J. Heat Transfer*, **113**, Nov., p.966 (1991).
8) K.Murata and K. Hashizume, *J. Heat Transfer*, **115**, Aug., p.680 (1993).
9) Sh.Koyama, J.Yu, S.Momoki, T.Fujii, and H.Honda, Proceeding of International Conference on Convective Flow Boiling, Banff, Canada, IV-3, 1995.
10) JAR, *Thermophysical Properties of Refrigerant: R22*, Japanese Association of Refrigeration, 1975.
11) JAR, *Thermophysical Properties of Environmentally Acceptable Fluorocarbons: HFC-134a and HCFC-123*, Japanese Association of Refrigeration, 1991.
12) D.S.Scott, Advances in Chemical Engineering (Academic Press, New York, 1963), **4**, p.200.
13) H.Takamatsu, S.Momoki and T.Fujii, *Int. J. Heat Mass Transfer*, **36, 13**, p.3351 (1993).

Appendix

Tables A-1, A-2 and A-3 list some typical experimental data of HFC134a, HCFC123 and HCFC22, respectively. These tables include the kind of refrigerant, flow condition, refrigerant mass velocity G_R, subsection number *No.*, vapor quality x, measured pressure P, calculated refrigerant bulk temperature T_{Rc}, inside surface temperatures T_{Wi}, heat flux of refrigerant side q, experimental heat transfer coefficient α_{exp}, the outside surface temperature T_{Wt}, T_{Wr}, T_{Wb} and T_{Wl} at the top, righthand side, bottom and lefthand side of the tube, respectively. The values in tables are representative ones taken at the central position of each subsection.

Table A-1 Experimental data of HFC134a.

No.	x	P MPa	T_{RC} ℃	T_{wi} ℃	q kW/m^2	α_{exp} kW/m^2K	T_{Wt}	T_{Wr}	T_{Wb}	T_{Wl}	No.	x	P MPa	T_{RC} ℃	T_{wi} ℃	q kW/m^2	α_{exp} kW/m^2K	T_{Wt}	T_{Wr}	T_{Wb}	T_{Wl}
							−℃−											−℃−			
Run: 3jun012, HFC134a, Counter Flow, $G_R=356.9kg/(m^2s)$											Run: 3jun222, HFC134a, Parallel Flow, $G_R=356.2kg/(m^2s)$										
1	.00	.6781	23.43	26.91	4.46	1.281	26.93	26.91	26.93	26.93	1	.00	1.2219	30.14	32.38	3.68	1.646	32.39	32.42	32.39	32.35
2	.00	.6780	24.56	27.42	3.07	1.072	27.37	27.44	27.48	27.43	2	.00	1.2217	30.94	32.26	3.75	2.855	32.07	32.30	32.43	32.27
3	.00	.6778	25.61	27.77	2.40	1.114	27.70	27.77	27.85	27.78	3	.01	1.2214	30.93	32.20	2.12	1.680	31.90	32.22	32.47	32.24
4	.02	.6776	25.60	26.85	4.22	3.378	26.58	26.92	27.08	26.89	4	.03	1.2211	30.92	32.16	5.04	4.084	31.98	32.19	32.39	32.13
5	.05	.6772	25.58	26.66	5.59	5.160	26.40	26.66	26.97	26.70	5	.06	1.2206	30.91	32.10	6.33	5.329	31.89	32.11	32.34	32.12
6	.08	.6764	25.54	26.69	7.28	6.372	26.51	26.57	26.91	26.85	6	.09	1.2198	30.88	32.14	8.49	6.750	31.98	32.17	32.39	32.14
7	.12	.6757	25.51	27.25	9.91	5.706	26.84	27.27	27.50	27.49	7	.14	1.2191	30.86	32.40	11.3	7.347	32.13	32.44	32.23	32.92
8	.18	.6743	25.44	27.25	12.6	6.965	27.09	27.29	27.48	27.29	8	.20	1.2179	30.82	32.28	14.9	10.21	32.42	32.13	32.58	32.18
9	.26	.6723	25.34	27.33	16.4	8.221	27.23	27.10	27.53	27.66	9	.28	1.2161	30.77	32.18	18.6	13.19	32.28	32.01	32.20	32.44
10	.37.	6703	25.24	27.07	22.9	12.54	27.08	27.11	27.36	27.00	10	.39	1.2144	30.71	32.62	24.3	12.75	33.03	32.36	32.71	32.65
11	.51	.6669	25.07	27.12	29.6	14.41	27.10	26.92	27.41	27.42	11	.52	1.2118	30.63	32.72	31.6	15.13	32.95	32.68	32.71	32.90
12	.70	.6621	24.83	27.18	43.6	18.47	26.96	27.31	27.49	27.49	12	.71	1.2083	30.52	32.43	47.1	24.67	32.46	32.45	32.72	32.65
13	.89	.6585	24.64	27.83	61.5	19.29	27.67	27.69	28.22	28.48	13	.90	1.2057	30.44	33.97	65.7	18.61	33.77	33.88	34.97	34.03
14	.99	.6561	24.52	43.70	25.9	1.352	43.98	40.64	44.82	45.65	14	.99	1.2040	30.38	51.41	23.1	1.101	50.92	51.19	52.09	51.72
Run: 2jul171, HFC134a, Counter Flow, $G_R=307.1kg/(m^2s)$											Run:2jul162, HFC134a, Parallel Flow, $G_R=310.5kg/(m^2s)$										
1	.00	.6540	23.84	25.40	3.16	2.033	25.32	25.41	25.46	25.44	1	.05	.6659	25.01	28.99	58.9	14.79	28.59	28.88	29.64	29.58
2	.00	.6538	24.40	25.40	3.24	3.227	25.11	25.47	25.64	25.44	2	.20	.6657	25.01	28.55	52.5	14.80	28.53	28.68	28.79	28.83
3	.02	.6536	24.39	25.27	2.96	3.357	24.95	25.28	25.56	25.33	3	.37	.6655	25.00	27.69	30.8	11.44	27.77	27.69	27.88	27.79
4	.04	.6533	24.37	25.14	4.06	5.268	24.93	25.18	25.40	25.12	4	.52	.6652	24.98	27.37	20.6	8.610	27.44	27.39	27.45	27.44
5	.07	.6528	24.35	25.08	4.96	6.795	24.83	25.06	25.41	25.08	5	.64	.6641	24.93	26.89	16.0	8.155	27.09	26.66	26.99	27.01
6	.10	.6522	24.32	25.23	6.56	7.179	24.97	25.11	25.57	25.36	6	.72	.6622	24.83	26.33	13.0	8.666	26.32	26.22	26.39	26.57
7	.15	.6515	24.28	25.65	8.45	6.170	25.24	25.43	25.69	26.36	7	.80	.6604	24.74	25.90	10.6	9.089	25.96	25.90	26.10	25.77
8	.21	.6504	24.23	25.59	11.4	8.351	25.52	25.30	25.99	25.69	8	.85	.6578	24.61	25.63	8.41	8.192	25.44	25.61	25.39	26.19
9	.29	.6489	24.15	25.44	14.6	11.25	25.47	25.20	25.51	25.76	9	.90	.6546	24.44	24.97	6.70	12.75	24.97	25.01	25.00	24.96
10	.39	.6474	24.07	25.80	19.5	11.30	26.05	25.59	25.90	25.87	10	.94	.6513	24.27	24.64	5.58	15.29	24.65	24.68	24.67	24.61
11	.53	.6448	23.94	25.64	26.2	15.40	25.73	25.62	25.71	25.81	11	.97	.6489	24.15	24.39	4.95	20.74	24.40	24.43	24.41	24.38
12	.73	.6413	23.75	25.58	38.2	20.92	25.63	25.52	25.84	25.79	12	.99	.6475	24.08	25.28	2.76	2.306	25.68	24.85	25.25	25.35
13	.92	.6386	23.61	29.77	52.9	8.584	30.71	29.47	29.40	30.15	13	1.00	.6461	24.45	26.38	1.13	5.855	26.39	26.41	26.40	26.34
14	1.00	.6368	26.54	47.61	17.9	0.849	47.44	47.58	47.53	48.09	14	1.00	.6447	24.98	26.42	1.22	0.849	26.42	26.43	26.42	26.42
Run: 3jun021, HFC134a, Counter Flow, $G_R=220.8kg/(m^2s)$											Run: 3jun243, HFC134a, Parallel Flow, $G_R=209.2kg/(m^2s)$										
1	.00	.6781	23.43	26.91	4.46	1.281	26.93	26.91	26.93	26.93	1	.04	.5709	19.94	22.67	36.1	13.23	22.34	22.51	23.10	23.15
2	.00	.6780	24.56	27.42	3.07	1.072	27.37	27.44	27.48	27.43	2	.18	.5703	19.90	22.33	33.1	13.61	22.13	22.44	22.67	22.48
3	.00	.6778	25.61	27.77	2.40	1.114	27.70	27.77	27.85	27.78	3	.34	.5694	19.85	21.71	20.0	10.74	21.52	21.77	22.10	21.70
4	.02	.6776	25.60	26.85	4.22	3.378	26.58	26.92	27.08	26.89	4	.49	.5681	19.78	21.43	14.4	8.724	21.47	21.55	21.62	21.26
5	.05	.6772	25.58	26.66	5.59	5.160	26.40	26.66	26.97	26.70	5	.60	.5665	19.69	21.08	11.6	8.344	21.09	21.23	21.28	20.87
6	.08	.6764	25.54	26.69	7.28	6.372	26.51	26.57	26.91	26.85	6	.70	.5645	19.57	20.48	9.35	10.36	20.48	20.42	20.53	20.58
7	.12	.6757	25.51	27.25	9.91	5.706	26.84	27.27	27.50	27.49	7	.77	.5625	19.46	20.08	7.47	12.00	20.14	20.10	20.07	20.10
8	.18	.6743	25.44	27.25	12.6	6.965	27.09	27.29	27.48	27.29	8	.83	.5605	19.34	19.82	6.37	13.39	19.78	19.84	19.86	19.86
9	.26	.6723	25.34	27.33	16.4	8.221	27.23	27.10	27.53	27.66	9	.88	.5584	19.22	19.43	4.39	20.80	19.50	19.44	19.42	19.43
10	.37	.6703	25.24	27.07	22.9	12.54	27.08	27.11	27.36	27.00	10	.91	.5563	19.10	19.27	3.89	23.68	19.25	19.29	19.32	19.24
11	.51	.6669	25.07	27.12	29.6	14.41	27.10	26.92	27.41	27.42	11	.95	.5545	19.00	19.14	3.32	24.18	19.11	19.15	19.15	19.17
12	.70	.6621	24.83	27.18	43.6	18.47	26.96	27.31	27.49	27.49	12	.97	.5531	18.92	19.07	3.14	20.94	19.08	19.08	19.09	19.06
13	.89	.6585	24.64	27.83	61.5	19.29	27.67	27.69	28.22	28.48	13	.99	.5520	18.85	19.60	3.15	4.208	19.58	19.34	19.16	20.36
14	.99	.6561	24.52	43.70	25.9	1.352	43.98	40.64	44.82	45.65	14	1.00	.5513	19.56	19.70	1.90	13.90	19.84	19.19	20.00	19.81

Table A-2 Experimental data of HCFC123.

No.	x	P MPa	T_{RC} °C	T_{wi} °C	q kW/m^2	α_{exp} kW/m^2K	T_{Wt}	T_{Wr}	T_{Wb}	T_{Wl}
							—°C—			
Run: 2feb211, HCFC123, Counter Flow, $G_R=309.0kg/(m^2s)$										
1	.00	.2695	53.41	59.23	3.39	0.582	59.11	59.24	59.31	59.31
2	.00	.2694	55.13	59.31	3.73	0.891	59.14	59.32	59.49	59.33
3	.00	.2693	57.89	59.31	3.68	2.589	59.07	59.37	59.55	59.31
4	.03	.2692	57.88	59.43	4.73	3.048	59.19	59.38	59.64	59.56
5	.06	.2685	57.79	59.56	4.85	2.748	59.28	59.50	59.94	59.57
6	.10	.2674	57.65	59.79	6.79	3.171	59.51	59.72	60.01	60.00
7	.16	.2662	57.50	59.93	8.52	3.500	59.80	59.87	60.03	60.14
8	.23	.2637	57.17	60.17	10.7	3.570	60.07	60.35	60.09	60.28
9	.32	.2597	56.65	59.79	14.2	4.505	59.93	59.67	59.87	59.88
10	.44	.2557	56.13	59.85	20.7	5.562	59.86	59.65	59.96	60.16
11	.62	.2518	55.60	59.38	30.1	7.943	59.39	59.67	59.31	59.51
12	.85	.2479	55.07	59.31	37.5	8.853	58.32	58.95	61.39	59.02
13	1.00	.2449	54.67	69.89	10.7	0.705	69.83	69.99	69.95	69.92
14	1.00	.2430	58.99	70.87	4.75	0.400	70.80	70.80	70.95	70.97
Run: 2feb251, HCFC123, Counter Flow, $G_R=304.9kg/(m^2s)$										
1	.00	.4549	70.02	77.95	6.20	0.782	77.92	77.95	77.99	78.01
2	.00	.4549	72.81	78.08	5.81	1.103	78.06	78.09	78.10	78.11
3	.00	.4548	76.50	78.27	4.65	2.625	78.17	78.28	78.43	78.27
4	.03	.4547	77.07	78.48	5.04	3.549	78.26	78.46	78.68	78.60
5	.07	.4542	77.02	78.65	5.92	3.640	78.35	78.68	79.01	78.63
6	.12	.4533	76.94	78.95	7.77	3.866	78.66	78.86	79.22	79.17
7	.19	.4524	76.86	79.10	10.4	4.670	78.97	79.06	79.16	79.33
8	.28	.4506	76.71	79.42	13.6	4.996	79.31	79.52	79.51	79.51
9	.40	.4479	76.48	79.30	16.3	5.767	79.41	79.25	79.32	79.43
10	.55	.4452	76.24	79.37	23.9	7.663	79.36	79.16	79.47	79.75
11	.76	.4420	75.96	79.39	32.7	9.543	79.51	79.68	79.30	79.47
12	.95	.4383	75.64	85.85	18.4	1.799	86.22	86.38	86.31	84.71
13	1.00	.4355	80.00	88.73	2.93	0.336	88.72	88.69	88.76	88.77
14	1.00	.4336	81.61	89.08	2.44	0.327	89.04	89.05	89.14	89.12
Run: 2feb221, HCFC123, Counter Flow, $G_R=112.7kg/(m^2s)$										
1	.00	.2537	47.98	55.83	3.96	0.505	55.86	55.78	55.88	55.83
2	.00	.2537	52.62	56.26	3.00	0.825	56.14	56.38	56.34	56.21
3	.01	.2537	55.86	56.59	2.06	2.829	56.44	56.58	56.80	56.55
4	.05	.2537	55.86	56.80	2.29	2.414	56.53	56.89	56.96	56.85
5	.10	.2536	55.85	56.85	3.01	3.016	56.65	56.76	57.34	56.67
6	.17	.2535	55.83	57.01	4.45	3.777	56.66	56.96	57.27	57.19
7	.27	.2534	55.82	57.27	5.54	3.797	57.00	57.10	57.51	57.56
8	.38	.2531	55.77	57.57	6.15	3.428	57.29	57.75	57.69	57.61
9	.53	.2525	55.70	57.41	10.2	5.965	57.25	57.42	57.75	57.36
10	.72	.2520	55.63	58.17	10.1	3.981	57.88	58.20	58.57	58.14
11	.89	.2513	55.54	60.98	7.22	1.326	61.01	61.41	58.29	63.30
12	.97	.2505	55.43	65.24	1.05	0.107	65.17	65.26	65.30	65.24
13	.98	.2499	55.35	65.57	0.27	0.027	65.61	65.50	65.58	65.59
14	.98	.2495	55.29	65.73	0.09	0.009	65.69	65.74	65.73	65.75

No.	x	P MPa	T_{RC} °C	T_{wi} °C	q kW/m^2	α_{exp} kW/m^2K	T_{Wt}	T_{Wr}	T_{Wb}	T_{Wl}
							—°C—			
Run: 3oct193, HCFC123, Parallel Flow, $G_R=293.2kg/(m^2s)$										
1	.00	.2795	50.45	61.67	16.9	1.507	61.54	61.55	61.82	61.97
2	.00	.2792	58.24	62.13	13.9	3.568	61.94	62.17	62.34	62.23
3	.05	.2787	59.08	61.93	9.60	3.362	61.70	61.85	62.38	61.93
4	.12	.2780	59.00	61.41	7.94	3.286	61.13	61.62	61.76	61.24
5	.17	.2768	58.84	61.04	7.24	3.296	60.90	61.08	61.40	60.84
6	.22	.2749	58.61	60.48	6.35	3.385	60.40	60.55	60.62	60.45
7	.27	.2731	58.37	60.06	5.93	3.519	60.03	60.09	60.17	60.00
8	.32	.2704	58.04	59.40	5.98	4.388	59.37	59.40	59.55	59.34
9	.36	.2669	57.59	58.78	5.63	4.760	58.82	58.91	58.76	58.69
10	.40	.2635	57.14	58.22	5.36	5.006	58.24	58.29	58.23	58.17
11	.45	.2596	56.63	57.75	5.30	4.736	57.79	57.77	57.77	57.74
12	.49	.2552	56.06	57.02	5.58	5.778	57.03	57.03	57.04	57.06
13	.52	.2519	55.62	56.70	6.34	5.907	56.62	56.74	56.80	56.69
14	.55	.2498	55.33	56.35	7.83	7.666	56.43	56.36	56.37	56.33
Run: 3oct131, HCFC123, Parallel Flow, $G_R=224.1kg/(m^2s)$										
1	.00	.2685	52.67	61.24	27.1	3.164	60.97	61.11	61.44	61.76
2	.08	.2678	57.71	61.40	23.5	6.369	61.10	61.52	61.78	61.47
3	.20	.2668	57.58	60.45	15.4	5.370	60.16	60.53	60.84	60.45
4	.33	.2655	57.41	59.73	11.3	4.879	59.54	59.81	59.99	59.70
5	.43	.2634	57.14	58.89	9.82	5.615	58.86	58.90	59.11	58.81
6	.52	.2606	56.76	57.95	8.13	6.874	57.94	57.91	57.97	58.07
7	.59	.2577	56.39	57.27	7.06	7.963	57.31	57.30	57.33	57.24
8	.66	.2544	55.95	56.48	6.66	12.52	56.38	56.53	56.61	56.48
9	.72	.2507	55.45	55.73	5.66	20.31	55.77	55.81	55.73	55.69
10	.77	.2470	54.95	55.12	4.64	27.22	55.12	55.19	55.16	55.08
11	.82	.2433	54.45	54.67	4.35	19.92	54.69	54.68	54.66	54.69
12	.86	.2397	53.95	54.06	4.11	36.27	54.04	54.10	54.05	54.10
13	.89	.2370	53.57	53.74	4.77	27.41	53.71	53.76	53.81	53.75
14	.91	.2352	53.31	53.50	5.12	28.06	53.53	53.52	53.51	53.49
Run: 3oct183, HCFC123, Parallel Flow, $G_R=143.7kg/(m^2s)$										
1	.00	.2567	50.76	58.61	16.4	2.089	58.33	58.58	58.74	58.97
2	.06	.2564	56.22	58.89	12.9	4.820	58.46	58.87	59.35	59.04
3	.18	.2561	56.17	58.15	9.75	4.931	57.80	58.09	58.75	58.08
4	.31	.2556	56.11	57.71	7.43	4.649	57.41	57.81	58.07	57.64
5	.41	.2548	56.01	57.36	6.67	4.935	57.15	57.61	57.65	57.11
6	.50	.2537	55.86	56.75	5.62	6.302	56.69	56.80	56.81	56.76
7	.58	.2526	55.70	56.31	4.93	8.203	56.24	56.32	56.46	56.27
8	.65	.2512	55.53	55.85	4.61	14.31	55.80	55.85	55.91	55.89
9	.72	.2497	55.32	55.47	3.72	24.68	55.44	55.52	55.51	55.46
10	.77	.2482	55.11	55.22	3.42	33.26	55.34	55.29	55.11	55.15
11	.81	.2468	54.93	55.01	2.55	30.80	55.10	55.01	55.00	54.97
12	.85	.2457	54.77	54.82	2.31	52.27	54.85	54.83	54.82	54.80
13	.88	.2448	54.65	54.86	2.08	10.16	54.87	54.77	54.76	55.07
14	.89	.2442	54.57	54.88	2.18	7.208	54.99	54.67	55.11	54.76

Table A-3 Experimental data of HCFC22.

No.	x	P MPa	T_{RC} °C	T_{wi} °C	q kW/m²	α_{exp} kW/m²K	T_{Wt}	T_{Wr}	T_{Wb}	T_{Wl}
							−°C−			
Run: 2jul222, HCFC22, Counter Flow, G_R=394.4(kg/m²s)										
1	.00	1.2219	30.14	32.38	3.68	1.646	32.39	32.42	32.39	32.35
2	.00	1.2217	30.94	32.26	3.75	2.855	32.07	32.30	32.43	32.27
3	.01	1.2214	30.93	32.20	2.12	1.680	31.90	32.22	32.47	32.24
4	.03	1.2211	30.92	32.16	5.04	4.084	31.98	32.19	32.39	32.13
5	.06	1.2206	30.91	32.10	6.33	5.329	31.89	32.11	32.34	32.12
6	.09	1.2198	30.88	32.14	8.49	6.750	31.98	32.17	32.39	32.14
7	.14	1.2191	30.86	32.40	11.3	7.347	32.13	32.44	32.23	32.92
8	.20	1.2179	30.82	32.28	14.9	10.21	32.42	32.13	32.58	32.18
9	.28	1.2161	30.77	32.18	18.6	13.19	32.28	32.01	32.20	32.44
10	.39	1.2144	30.71	32.62	24.3	12.75	33.03	32.36	32.71	32.65
11	.52	1.2118	30.63	32.72	31.6	15.13	32.95	32.68	32.71	32.90
12	.71	1.2083	30.52	32.43	47.1	24.67	32.46	32.45	32.72	32.65
13	.90	1.2057	30.44	33.97	65.7	18.61	33.77	33.88	34.97	34.03
14	.99	1.2040	30.38	51.41	23.1	1.101	50.92	51.19	52.09	51.72
Run: 2feb021, HCFC22, Counter Flow, G_R=306.1(kg/m²s)										
1	.00	.9980	20.02	24.71	9.49	2.022	24.57	24.70	24.85	24.85
2	.00	.9979	23.33	24.95	8.10	5.026	24.77	24.89	25.35	24.87
3	.04	.9978	23.33	24.76	7.94	5.546	24.29	24.71	25.21	24.93
4	.09	.9976	23.32	24.85	9.82	6.413	24.53	24.75	25.18	25.07
5	.15	.9969	23.30	24.91	12.4	7.650	24.69	24.89	25.35	24.86
6	.24	.9957	23.25	25.00	16.2	9.275	24.69	25.09	25.04	25.37
7	.35	.9945	23.21	25.11	21.0	11.06	24.97	25.18	24.97	25.58
8	.49	.9925	23.13	25.30	27.1	12.52	24.94	26.48	24.93	25.16
9	.67	.9897	23.03	24.93	33.9	17.85	25.22	24.81	25.12	24.97
10	.87	.9869	22.93	26.35	32.8	9.591	26.33	26.94	26.44	26.09
11	.99	.9848	22.85	38.77	6.13	0.385	38.73	38.87	38.82	38.72
12	1.00	.9834	25.97	39.87	3.25	0.234	39.85	39.91	39.92	39.83
13	1.00	.9823	28.34	40.39	1.04	0.086	40.39	40.37	40.38	40.41
14	1.00	.9816	29.96	40.62	4.51	0.423	40.56	40.61	40.72	40.65
Run: 2jul221, HCFC22, Counter Flow, G_R=207.8(kg/m²s)										
1	.00	1.0421	24.45	26.12	2.60	1.551	26.15	26.15	26.12	26.11
2	.01	1.0421	24.93	25.76	2.35	2.844	25.53	25.81	25.95	25.77
3	.02	1.0420	24.93	25.63	2.56	3.651	25.28	25.67	25.92	25.68
4	.05	1.0419	24.92	25.53	3.40	5.574	25.27	25.60	25.75	25.54
5	.08	1.0417	24.92	25.46	4.42	8.108	25.23	25.51	25.74	25.42
6	.13	1.0415	24.91	25.45	5.54	10.27	25.25	25.46	25.71	25.42
7	.19	1.0413	24.90	25.73	7.69	9.241	25.35	25.68	25.79	26.19
8	.26	1.0409	24.89	25.64	9.27	12.31	25.59	25.55	25.89	25.64
9	.36	1.0403	24.87	25.65	12.3	15.72	25.58	25.47	25.81	25.87
10	.47	1.0397	24.85	25.95	14.8	13.44	26.06	25.75	26.15	26.01
11	.63	1.0388	24.81	25.89	20.4	18.82	25.96	25.74	26.07	26.03
12	.83	1.0374	24.76	26.01	25.4	20.33	25.91	26.02	26.11	26.30
13	.98	1.0364	24.73	35.67	16.2	1.479	38.76	33.38	38.84	31.89
14	1.00	1.0357	28.34	40.85	4.62	0.370	40.94	40.84	40.71	40.96

No.	x	P MPa	T_{RC} °C	T_{wi} °C	q kW/m²	α_{exp} kW/m²K	T_{Wt}	T_{Wr}	T_{Wb}	T_{Wl}
							−°C−			
Run: 2feb154, HCFC22, Counter Flow, G_R=115.3(kg/m²s)										
1	.00	.6627	3.22	9.91	3.03	0.452	10.02	9.92	9.84	9.91
2	.00	.6614	6.71	9.93	3.10	0.962	9.62	10.08	10.15	9.93
3	.01	.6595	8.94	9.71	2.25	2.923	9.37	9.74	9.86	9.91
4	.05	.6570	8.82	9.67	3.05	3.594	9.29	9.72	9.72	9.98
5	.10	.6558	8.76	9.65	3.31	3.706	9.52	9.46	9.77	9.90
6	.16	.6559	8.76	9.70	4.44	4.734	9.61	9.43	9.90	9.93
7	.23	.6560	8.77	9.92	5.78	5.004	9.49	9.50	10.13	10.63
8	.32	.6559	8.76	9.80	6.55	6.305	9.76	9.82	9.74	9.95
9	.43	.6557	8.75	9.70	8.70	9.106	9.52	9.54	9.81	10.05
10	.58	.6554	8.74	10.04	10.8	8.307	10.09	9.79	10.03	10.36
11	.77	.6551	8.72	10.06	15.2	11.37	10.20	9.84	10.02	10.36
12	.92	.6549	8.71	18.70	5.28	0.529	17.00	22.72	24.07	11.06
13	.98	.6546	8.70	25.51	6.00	0.357	25.44	25.61	25.89	25.15
14	1.00	.6545	9.47	26.06	1.78	0.107	25.93	26.17	26.41	25.74
Run: 2jul212, HCFC22, Parallel Flow, G_R=311.8(kg/m²s)										
1	.06	1.1203	27.63	30.35	58.0	21.37	29.96	30.24	30.87	31.02
2	.21	1.1194	27.60	29.97	52.6	22.18	29.92	30.09	30.20	30.31
3	.38	1.1181	27.56	29.12	30.8	19.68	29.12	29.15	29.40	29.19
4	.53	1.1163	27.50	28.84	20.8	15.61	28.90	28.84	28.94	28.91
5	.64	1.1142	27.43	28.65	16.4	13.45	28.75	28.60	28.78	28.65
6	.73	1.1116	27.34	28.34	12.7	12.76	28.41	28.26	28.35	28.49
7	.80	1.1090	27.25	28.10	10.4	12.29	28.13	28.06	28.32	28.00
8	.85	1.1064	27.16	27.97	8.12	10.13	27.76	27.99	27.76	28.45
9	.90	1.1037	27.07	27.43	6.30	17.77	27.43	27.48	27.47	27.40
10	.93	1.1010	26.98	27.18	5.20	26.00	27.20	27.23	27.21	27.14
11	.96	1.0987	26.90	27.04	4.42	31.26	27.06	27.12	27.05	26.99
12	.99	1.0969	26.84	26.96	3.82	31.96	26.86	26.94	27.14	26.94
13	1.00	1.0955	26.83	27.07	2.69	11.26	27.04	27.33	27.07	26.88
14	1.00	1.0946	28.33	28.28	2.81	* * *	28.24	28.35	28.27	28.28
Run: 2jul213, HCFC22, Parallel Flow, G_R=200.4(kg/m²s)										
1	.07	1.1273	27.87	30.27	37.5	15.62	29.97	30.08	30.65	30.83
2	.22	1.1269	27.86	29.86	34.3	17.14	29.70	29.98	30.12	30.03
3	.39	1.1263	27.84	29.14	20.4	15.73	28.99	29.21	29.48	29.10
4	.55	1.1255	27.81	28.90	13.9	12.82	28.84	28.94	29.08	28.90
5	.66	1.1246	27.78	28.78	11.1	11.05	28.81	28.79	28.92	28.74
6	.76	1.1236	27.75	28.50	8.88	11.81	28.51	28.51	28.53	28.55
7	.83	1.1226	27.71	28.25	7.18	13.46	28.27	28.28	28.42	28.10
8	.89	1.1216	27.68	28.15	5.71	12.13	28.00	28.17	28.02	28.48
9	.94	1.1206	27.64	27.82	4.40	25.06	27.82	27.87	27.84	27.79
10	.97	1.1196	27.61	27.70	3.46	38.93	27.70	27.71	27.74	27.69
11	1.00	1.1187	27.58	29.23	1.21	0.735	29.21	29.16	29.25	29.30
12	1.00	1.1181	28.05	29.41	0.43	0.311	29.40	29.43	29.42	29.41
13	1.00	1.1176	28.51	29.52	0.18	0.181	29.51	29.54	29.50	29.52
14	1.00	1.1173	28.97	29.51	0.92	1.704	29.50	29.53	29.51	29.51